Detecting and controlling unstable periodic orbits that are not part of a chaotic attractor

Matjaž Perc and Marko Marhl*
Department of Physics, Faculty of Education, University of Maribor, Koroška cesta 160, SI-2000 Maribor, Slovenia
(Received 14 October 2003; published 12 July 2004)

A method for controlling unstable periodic orbits (UPOs) that have not been controllable before is presented. The method is based on detecting UPOs that are situated outside the skeleton of a chaotic attractor. The main idea is to exploit flexible parts of the attractor, which under weak external perturbations allow variable excursions of the trajectory away from its originally determined path. After the perturbation, the trajectory of the autonomous system seeks its path back to the chaotic attractor and reveals additional UPOs that are otherwise not used by the system. It is shown that these UPOs can be controlled as easily as the UPOs that form the basic chaotic attractor. The effectiveness of the proposed method is demonstrated on two different chaotic systems with very distinct response abilities to external perturbations. Additionally, some applications of the method in the fields of laser technology, information encoding, and biomedical engineering are discussed.

DOI: 10.1103/PhysRevE.70.016204 PACS number(s): 05.45.Gg, 82.40.Bj

I. INTRODUCTION

Deterministic chaotic systems are by definition extremely sensitive to changes in initial conditions. This implies that the distance between two trajectories emerging from nearly identical initial conditions grows exponentially in the course of time. Since in real-life systems, initial conditions are never known perfectly, it is impossible to predict the exact evolution of a chaotic system. The most prominent example of such a chaotic system is the weather, which can be, in a simple form, modeled by the well-known Lorenz equations [1].

Another important property of chaotic systems, besides there extreme sensitivity to changes in initial conditions, is that the skeleton of every chaotic attractor consists of infinitely many unstable periodic orbits (UPOs). Since the dynamics of a chaotic attractor is ergodic the neighborhood of every point in each one of the UPOs is ergodically visited by the trajectory during the temporal evolution of the system. Consequently, the dynamics of a chaotic system can be seen as constantly shadowing some periodic behavior, erratically jumping from one UPO to another. This fact, combined with the extreme sensitivity of a chaotic system to small perturbations, led to the idea of chaos control.

The first algorithm for controlling UPOs embedded within the chaotic attractor was conceived more than a decade ago at the University of Maryland [2]. The main idea of the method is to wait for a natural passage of the trajectory close to the desired periodic behavior and then judiciously perturb a system parameter in order to stabilize the chosen, initially unstable, periodic orbit. Later on, several other methods for controlling UPOs embedded within the chaotic attractor were proposed. Among them were the occasional proportional feedback method proposed by Hunt [3], the delayed feedback method proposed by Pyragas [4], the adaptive method proposed by Boccaletti and Arecchi [5], and the method proposed by Plapp and Huebler [6], which consists of constructing control forces based upon the knowledge of the model equations and the goal dynamics. All these methods belong to the so-called closed loop or feedback methods, which have the property that their action is completely goal oriented and thus the outcome is exactly known. On the other hand, there exist the so-called open loop or non feedback methods. These strategies consider the effects of external perturbations, such as periodic inputs [7,8] or noise [9], on the evolution of a chaotic system. Unlike the closed loop methods, the outcome of the open loop methods is not known, thus their action is not goal oriented in the sense that the exact output dynamics cannot be predicted. Nevertheless, in our previous paper we showed that with certain periodic forcing, the frequency of the resulted system state can be precisely defined and controlled [8].

The strategies for chaos control were recently enhanced and applied to nonautonomous systems [10–12]. Gammaitoni *et al.* [10], for example, used an open-loop control scheme in order to enhance or suppress the spectral response of threshold-crossing events triggered by a time-periodic signal in background noise. Later on, several other external feedback strategies were analyzed for their effectiveness in enhancing or depressing natural stochastic resonance effects [11]. In particular, these noninvasive control techniques were recognized to be especially valuable for noisy bistable systems that are difficult or impossible to modify internally. Moreover, possible applications of these results for the effect of synchronization control were discussed in [12].

In the present paper, we extend the applicability of chaos control techniques by introducing a method that enables the control of UPOs that have not been controllable before. The presented method reveals additional UPOs that are not part of the basic chaotic attractor, but which can be controlled as easily as the UPOs that form the skeleton of the chaotic attractor. These UPOs extend the richness of dynamical states that are available for control. The main virtue of controlling chaotic systems is the permanent accessibility of infinitely many dynamical states that are incorporated in a chaotic attractor. However, these dynamical states usually differ

*Corresponding author. Email address: marko.marhl@uni-mb.si

from one another very little and thus the true richness of the available dynamics is often not as prospective as one would expect. For example, in chaotic regimes that emerge via the period doubling root, only period one, period two, etc., cycles differ from one another considerably, whereas all other UPOs more or less resemble them, i.e., have nearly the same shape and frequency of oscillations as the integer multiples. This fictitious richness of diverse dynamical states is even more expressed in intermittent chaotic systems that behave almost regularly with only intermittently occurring deviations [13]. Therefore, particularly in such cases, our method can greatly increases the repertoire of genuinely diverse dynamical states and can thereby extend the applicability of chaos control techniques.

The main idea of our method is to achieve an excursion of the trajectory away from its originally determined path with a short pulsatile external forcing. Afterwards, the autonomous system reveals additional UPOs as it resettles onto the basic chaotic attractor. The virtue of the method lies in the fact that when resettling and revealing additional UPOs the system is not subjected to any external influences, i.e., it is completely autonomous, and therefore these UPOs can be controlled as easily as the unstable periodic orbits that are a part of the basic chaotic attractor. Due to the noninvasive nature, our method is particularly valuable for chaotic systems that are difficult or impossible to modify internally, i.e., with hard parameter changes. Our method is noninvasive in so far that additional UPOs can be detected without changing the internal parameter values of the system. We demonstrate the effectiveness of the method on a particular mathematical model for intracellular Ca^{2+} oscillations [14] that for certain parameter values exhibits intermittent chaotic behavior [13]. Hence, the frequency interval that contains all UPOs that form the skeleton of the chaotic attractor is rather narrow. Especially in such cases, the proposed method can largely expand the frequency interval of UPOs without modifying internal parameters of the system.

It should be noted that the proposed method exploits flexible parts of the chaotic attractor, which under weak external perturbations enable considerable deviations of the trajectory away from its originally determined path. Therefore, the multitude of additional UPOs that exist outside the skeleton of a chaotic attractor can be predicted, i.e., estimated in advance. In our previous studies we showed that the local divergence, calculated along the trajectory, largely determines the flexibility of the corresponding attractor [15–17]. We found that close to zero local divergence characterizes flexible attractors, whereas highly negative local divergence is a characteristic property of very rigid systems. Here, we show that the flexibility of a particular chaotic regime can be used to estimate the richness of additional UPOs that exists outside the skeleton of a chaotic attractor. We emphasize that flexible chaotic attractors possess many more additional UPOs, i.e., UPOs that do not form the basic skeleton, than do rigid chaotic regimes. In order to demonstrate this, we apply the method to another mathematical model [18] in which very rigid chaotic regimes can be found. We show that in this case, additional UPOs can be found only in a moderate extension of the frequency interval that contains all UPOs of the basic chaotic attractor.

The paper is structured as follows. Section II is devoted to the description of mathematical methods used for the bifurcation analysis, determination of flexibility and robustness, as well as methods for detecting and controlling UPOs. In particular, is method, which enables us to detect and control additional UPOs that have not been controllable before, is pointed out. In Sec. III we present the results, and in the last section we discuss the merits and limitations of our method. Some applications of the method in the fields of laser technology, information encoding, and biomedical engineering are also discussed. Mathematical models with complete sets of model equations and parameter values are given in Appendices A and B.

II. METHODS

A. Bifurcation analysis

The bifurcation analysis was carried out by the continuation software AUTO97 [19]. In addition to the bifurcation analysis of the whole system, a method proposed by Rinzel [20] was used. This method can only be applied to systems, which can be separated into a fast and a slow subsystem. Therefore, we refer to it as the fast-slow subsystem analysis. Each variable that changes rapidly in time is a part of the fast subsystem, whereas the variables that vary slowly represent the slow subsystem. The bifurcation analysis of the fast subsystem, whereby taking the variables of the slow subsystem as bifurcation parameters, gives evidence of local properties of the trajectory in the complete phase space.

B. Determining flexibility and robustness of dynamical systems

Flexibility and robustness are very important properties of dynamical systems since they constitute the response abilities of a system to various external perturbations, such as periodic functions [8,21], steplike forcing [15], and noise [16]. Let us consider a dissipative dynamical system

$$\frac{d\mathbf{x}}{dt} = \mathbf{F}(\mathbf{x}, \mu), \tag{1}$$

where $\mathbf{x}=(x_1, x_2, \ldots, x_i, \ldots, x_D)$ and $\mathbf{F}=(F_1, F_2, \ldots, F_i, \ldots, F_D)$ are a D-dimensional vector and the governing vector field, respectively, and μ is a set of fixed control parameters. Previously, we showed that the local divergence of the vector field $\mathbf{F}$, calculated according to the equation

$$\nabla \cdot \mathbf{F} = \frac{\partial F_1}{\partial x_1} + \frac{\partial F_2}{\partial x_2} + \cdots + \frac{\partial F_i}{\partial x_i} + \cdots + \frac{\partial F_D}{\partial x_D}, \tag{2}$$

is the crucial system property that determines the flexibility and robustness of a dynamical system [15,17]. The local divergence determines attraction properties of an attractor at a given point. Therefore, extensive close to zero local divergence parts largely facilitate response abilities of the system and characterize flexible systems, whereas on the other hand, highly negative local divergence areas characterize very rigid dynamical states that are almost impossible to modify even with strong external signals.

C. Adaptive method for chaos control

The control of UPOs was carried out with the algorithm proposed by Boccaletti and Arecchi [5], which is based on the delayed feedback method originally proposed by Pyragas [4]. Here, we will briefly summarize the algorithm, whereas its complete description can be found in [5,22–24]. In order to determine the period of a particular UPO embedded in the attractor, the algorithm exploits local expansion and contraction rates of a dynamical system, which are calculated according to the equation

$$\lambda_i(t_{n+1}) = \frac{1}{\tau_n}\ln\left|\frac{x_i(t_{n+1}) - x_i(t_n)}{x_i(t_n) - x_i(t_{n-1})}\right|, \tag{3}$$

where τ_n is the minimum of all $\tau_n^{(i)}$ calculated for all i dimensions of the dynamical system according to the equation

$$\tau_{n+1}^{(i)} = \tau_n^{(i)}\{1 - \tanh[\sigma\lambda_i(t_{n+1})]\}, \tag{4}$$

where σ is a strictly positive constant chosen in such a way as to forbid $\tau_{n+1}^{(i)}$ from going to zero. On this basis a sequence of observation time intervals (τ_n) is obtained, which enables us to determine the periods of UPOs embedded within the chaotic attractor. This is done by constructing return maps τ_{n+k} versus τ_n for $k=1,2,3,\ldots$ and calculating the rms error (η) of the point distribution around the diagonal for each k. With increasing k, the correlation between two successive τ_n decreases and thus $\eta(k)$ is a predominantly increasing function. More precisely, whenever the trajectory of the system shadows the neighborhood of a particular UPO, the correlation is rebuilt, which manifests as a local minimum of the function $\eta(k)$. For example, if the trajectory gets close to an UPO of period T, the function $\eta(k)$ has a local minimum at $k=T/\overline{\tau}$, where $\overline{\tau}$ is the average value of all τ_n. After determining the period of a particular UPO embedded within the chaotic attractor, the latter can be stabilized by introducing a correction term $(\mathbf{U})$ to each of the D differential equations of the system. The relative weight of the correction term applied to a particular differential equation of the system, i.e., U_i, where $\mathbf{U}=(U_1,U_2,\ldots,U_i,\ldots,U_D)$, is calculated according to the equation

$$U_i(t_{n+1}) = \frac{1}{\tau_n}[x_i(t_{n+1} - T) - x_i(t_{n+1})], \tag{5}$$

where each τ_n is calculated according to Eq. (4), whereas the local expansion and contraction rates are, for the purpose of chaos control, calculated with respect to a particular UPO that was chosen to be stabilized according to the equation

$$\lambda_i(t_{n+1}) = \frac{1}{\tau_n}\ln\left|\frac{x_i(t_{n+1}) - x_i(t_{n+1} - T)}{x_i(t_n) - x_i(t_n - T)}\right|. \tag{6}$$

Note that these local variation rates also determine the time interval during which the correction term has a constant value, thereby reflecting the necessity to perturb the dynamics more or less often in order to stabilize the desired UPO.

D. Method for detecting UPOs outside the skeleton of a chaotic attractor

On the basis of our previous studies regarding flexibility and robustness of dynamical systems [8,15–17,21] we here introduce a method for detecting additional UPOs that are not part of the basic chaotic attractor. The method exploits flexible regions of the attractor by perturbing the path of the trajectory so that it leaves the skeleton of the basic chaotic attractor and after the excursion resettles onto the attractor, thereby using regions of the phase space that are normally not visited by the unperturbed dynamics. With this procedure, UPOs that lie outside the skeleton of the basic chaotic attractor become visible and as such available for control. We detect UPOs by perturbing one of the fast variables of the system with a steplike flux, characterized by randomly selected intervals (h), duration (d), and amplitude (a), given by the function

$$f(t) = \begin{cases} a, & \text{if} \quad t \bmod h \geqslant h - d \\ -a, & \text{if} \quad (t-d) \bmod h \geqslant h - d \\ 0, & \text{else.} \end{cases} \tag{7}$$

$f(t)$ is a symmetric function, which for large enough h, and small enough d and a assures that the trajectory, after the perturbation and before completely resettling onto the attractor, is completely determined by the autonomous, i.e., unperturbed dynamical system. All three parameters that define the perturbation (h, d, and a) are chosen randomly within given ranges. This enables highly variable perturbing of the basic system and herewith the most efficient exploiting of all flexible areas of the studied chaotic regime. The trajectory herewith, after the perturbation and before completely resettling onto the attractor, reveals as many new UPOs as possible. Parameters h, d and a have to be chosen carefully, with respect to the system's dynamics. Parameter h has to be large enough in order to allow the trajectory to resettle onto the attractor before the next perturbation takes place. Parameters d and a determine how strong the path of the trajectory will be perturbed. It should be noted that for each particular d only one a is randomly selected. In practice some testing and experience with the studied dynamical system is necessary in order not to collapse the whole system, but nevertheless achieving large enough perturbations to prevent the trajectory to resettle onto the attractor immediately. As already noted in the subsection B, the local divergence [see Eq. (2)] of attractors in the phase space is an appropriate indicator for the system susceptibility to external perturbations and thus helps to determine parameters d and a.

III. RESULTS

For the mathematical model proposed by Marhl *et al.* [14], we first demonstrate the standard procedure of recognizing and controlling UPOs as described in subsection C. Since the biological particularities of the model are not of particular interest in this paper, the model is not described in detail. However, the complete set of model equations and parameter values is given in Appendix A, whereas a detailed analysis of the system's dynamics can be found in

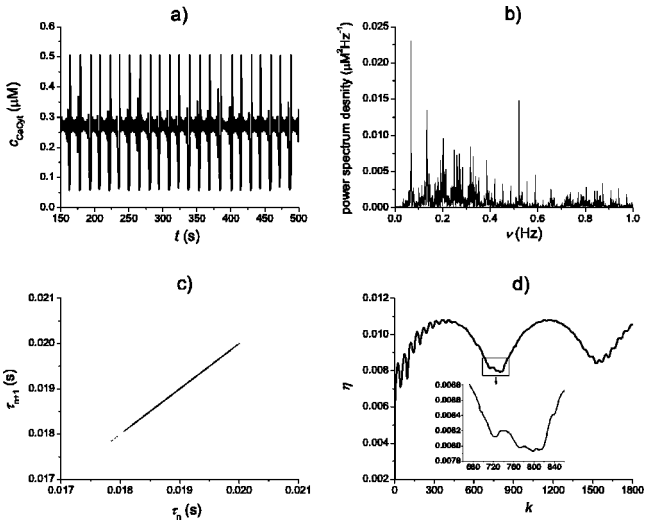

FIG. 1. Analysis of the basic chaotic regime with the adaptive recognition method. For equations and parameter values see Appendix A. (a) Time series of c_{CaCyt}. (b) Corresponding power spectra. (c) Return map of the observation times τ_{n+1} vs τ_n. (d) The rms error $\eta(k)$ of the point distribution around the diagonal for return maps τ_{n+k} vs τ_n.

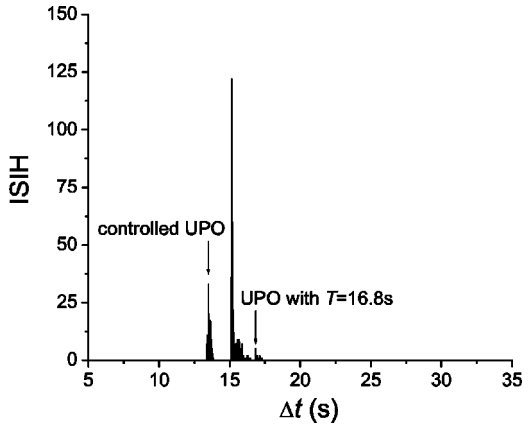

FIG. 2. Normalized ISIH of the c_{CaCyt} time series for the basic chaotic regime. For equations and parameter values, see Appendix A.

[13,14,25,26]. For the parameter values listed in Appendix A, the dynamical system exhibits intermittent chaotic oscillations, as shown in Fig. 1(a). This can also be well observed in the power spectra presented in Fig. 1(b), where the predominant oscillation frequency with its higher harmonics is well expressed.

In order to determine the periods of UPOs embedded within the chaotic attractor, we make use of the algorithm described in subsection C. Figure 1(c) shows the return map τ_{n+1} versus τ_n of the obtained observation times, which in this case have an average value $\overline{\tau}=0.0189$ s. The correlation between two successive τ_n is well expressed since all points cluster along the diagonal. In this case, $\eta(k)$ of the point distribution around the diagonal is nearly zero. However, as k increases the correlation between τ_{n+k} and τ_n decreases, which results in an increase of η. Nevertheless, there exist local minima at each k for which the examined chaotic regime has an UPO with the period $T=k\overline{\tau}$, as shown in Fig. 1(d). Note that the first few minima below $k=500$ correspond to shadowing the small-amplitude spikes between two main successive spikes of the system [see Fig. 1(a)] and cannot be taken as UPOs. We should focus on the well-expressed minimum at $k\approx 790$, which indicates that the system has a predominant oscillation period $T\approx 15$ s. This is fully in agreement with the power spectrum in Fig. 1(b), which has the main spike at $\nu=0.067$ Hz. By enlarging the area around $k\approx 790$ [see insert of Fig. 1(d)], we can determine the periods of UPOs embedded within the chaotic attractor, which range between ≈ 13 and 16 s.

In order to determine the periods of UPOs embedded within the chaotic attractor even more accurately, we calculate the normalized interspike interval histogram (ISIH) of the chaotic time series presented in Fig. 1(a). It is important to note that the ISIH can be used to extract periods of UPOs embedded in the chaotic attractor only if the UPOs are separated by well-expressed terminates, like main spikes in our case [see Fig. 1(a)]. In general, such oscillation patterns are characteristic for intermittent chaotic systems, whereas for period doubling chaos this is often not the case, i.e., it is impossible to determine where one UPO ends and the other starts by simply looking at the oscillations or calculating the distance between consecutive spikes.

The ISIH for the time series in Fig. 1(a) is presented in Fig. 2 and was calculated for approximately 10 000 main spikes. The histogram is fully in agreement with Fig. 1, showing that the predominant oscillation frequency of the system is $T\approx 15$ s, and the span of oscillation periods of all UPOs embedded within the chaotic attractor ranges between ≈ 13.4 and 16.9 s in a noncontinuous manner, i.e., for example, there does not exist an UPO within the chaotic attractor that has an oscillation period of 13.8 s$<T<$14.6 s. This also matches with the results obtained by the function $\eta(k)$ in Fig. 1, which does not have a local minimum of $719<k<775$ [see inset of Fig. 1(d)]. Moreover, in addition to $\eta(k)$, the ISIH provides more accurate information about the precise periods of UPOs embedded within the chaotic attractor, and it also shows how frequently a particular UPO occurs during the simulation time. The latter information is not explicitly provided by $\eta(k)$. Therefore, UPOs that are rare can remain completely undetected by the adaptive recognition method. For example, UPOs that have $T>16$ s occur rather rarely; therefore, they were not detected by the adaptive recognition method.

To demonstrate the effectiveness of the adaptive method for chaos control, we select an UPO with $T=13.5$ s, which is marked by the left arrow in Fig. 2. Note that the period of the chosen UPO occurs frequently but is nevertheless not the most dominant one. The results of the UPO control are presented in Fig. 3. It can be well observed that the system can be easily forced to shadow the selected UPO. The maximal required correction flux U_1 is three orders of magnitude smaller than the total dc_{CaCyt}/dt flux (not shown), which is in best agreement with other theoretical studies demonstrating the delayed feedback control of UPOs [3–6]. Moreover, the corrections are rarely required, i.e., only at the main c_{CaCyt} spikes (there the flux dc_{CaCyt}/dt is maximal), whereas during

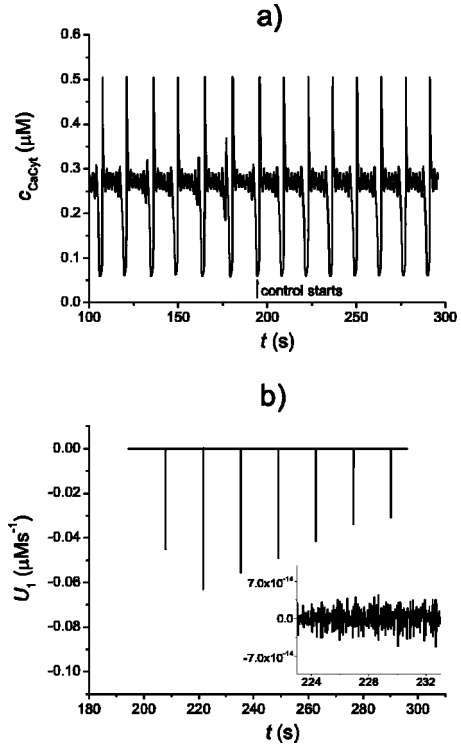

FIG. 3. Control of the unstable periodic orbit marked with the left arrow in Fig. 2. For equations and parameter values, see Appendix A. (a) Time series of c_{CaCyt}. (b) The corrections required for controlling the desired UPO.

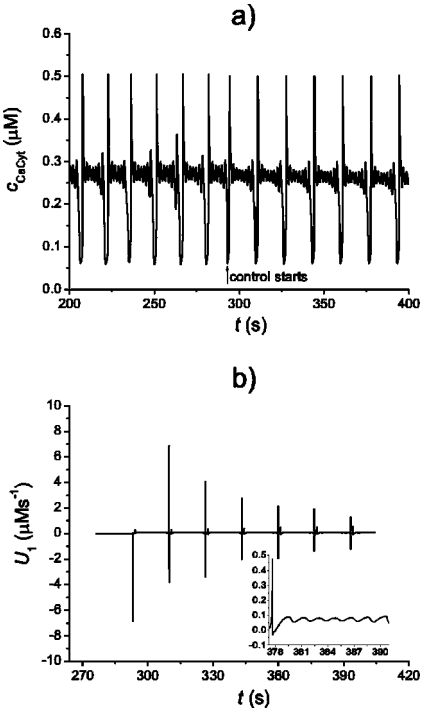

FIG. 4. Control of a periodic orbit obtained by changing the system parameters. For equations and parameter values see Appendix A. (a) Time series of c_{CaCyt}. (b) The corrections required for forcing the basic chaotic system to shadow the desired periodic orbit.

the small-amplitude spikes the required corrections are much smaller, as shown in the inset of Fig. 3(b).

For comparison, we force the basic chaotic system (parameter values as in Appendix A) to shadow the trajectory that has the same oscillation period as one of the UPOs ($T=16.8$ s, which is marked by the right arrow in Fig. 2) and lies physically within the region of the chaotic attractor; however, it is not a part of the attractor. The orbit was obtained by changing the following parameters: $k_{\mathrm{ch}}=4285\ \mathrm{s}^{-1}$, $k_m=0.006625\ \mathrm{s}^{-1}$, and $k_{\mathrm{out}}=132.5\ \mathrm{s}^{-1}$. Figure 4 shows that in this case it is also principally possible to slave the system to shadow the desired periodic orbit, however, the correction fluxes required to achieve this are very large and reach values up to the same order of magnitude as the total dc_{CaCyt}/dt flux. Moreover, the corrections needed to slave the dynamics are very large also in regions between the main spikes [see inset of Fig. 4(b)], especially when compared to the corrections required for slaving the dynamics to shadow one of the UPOs that form the basic skeleton of the chaotic attractor [see inset of Fig. 3(b)].

The above analysis shows that the periods of UPOs, embedded in the chaotic attractor of the examined dynamical system, are all confined to a rather narrow interval that ranges from approximately 13.4 to 16.9 s (see Fig. 2). Furthermore, we showed that any other randomly selected orbit obtained with hard parameter changes, even with the same oscillation period as one of the UPOs embedded in the chaotic attractor, cannot be easily controlled (see Fig. 4), i.e., such a trajectory cannot be considered as an UPO of the given chaotic system. However, in the following we will show that in fact the examined dynamical system possesses additional UPOs that are not part of the basic chaotic attractor but can be controlled as easily as those embedded in the chaotic attractor. In order to make these additional UPOs visible and available for control, we will deploy the method described in subsection D.

For the model studied here [14] we take, in accordance with Eq. (7), the following intervals from which h, d, and a are chosen randomly: $80\ \mathrm{s}<h<120\ \mathrm{s}$, $0\ \mathrm{s}<d<1\ \mathrm{s}$, and $0\ \mu\mathrm{M\ s}^{-1}<a<1\ \mu\mathrm{M\ s}^{-1}$. To present and explain the effects of the external perturbation we carry out the bifurcation analysis using the fast-slow subsystem analysis as described in subsection A. In the examined dynamical system, the fast changing variables were identified to be c_{CaCyt} and c_{CaEr}, whereas the slow changing variable, which is used as the bifurcation parameter, is c_{CaMit}. The obtained bifurcation diagrams for the unperturbed and perturbed dynamics, together with the two-dimensional (2D) projection of the trajectory in the whole phase space, are presented in Figs. 5(a) and 5(b), respectively. Note that the 2D projection of the whole phase space for the perturbed dynamics does not contain those oscillation cycles that were directly perturbed by $f(t)$; thus, only those oscillation cycles were considered that were obtained by resettling of the trajectory onto the chaotic attractor. The solid line represents stable foci; the dashed line represents unstable foci, whereas the dash-dotted lines that emerge out of the supercritical Hopf bifurcation (HB) represent stable periodic orbits. In the bifurcation diagram of the unperturbed dynamics a very important system property can be well observed, namely, the slow passage effect

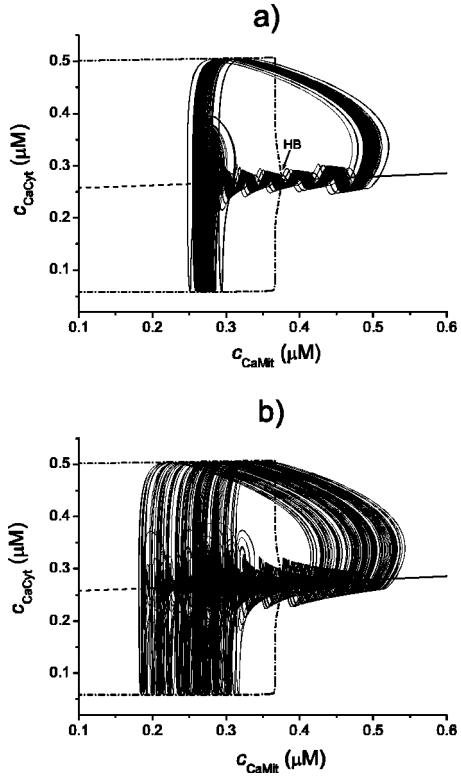

FIG. 5. Bifurcation diagram obtained with the fast-slow subsystem analysis together with the 2D projection of the trajectory in the whole phase space. HB denotes the Hopf bifurcation. For equations and parameter values see Appendix A. (a) Basic chaotic regime. (b) Basic chaotic regime with the applied method for revealing additional UPOs.

[25,27–30]. The latter manifests as a delayed transition of the trajectory to the lower stable periodic branch after the supercritical Hopf bifurcation is exceeded in the clockwise direction. Despite the fact that the stable foci branch turns unstable after the supercritical HB is exceeded, the trajectory remains close to the rest state for a considerable amount of time before it unfolds to the lower stable periodic branch, which is a clear indicator for the slow passage effect.

The most characteristic property of the slow passage effects is its extreme sensitivity to external perturbations. Several authors have reported that the length of the slow passage phase can be altered by any kind of external perturbations, such as stochastic influences and periodic environmental perturbations [27] or external influences from neighboring oscillators [31–33], and even by precision of numerical algorithms used for integration of differential equations [34]. Recently, we proposed a more general view, showing that the local divergence represents the key system property that determines sensitivity of dynamical systems to external perturbations [35]. We showed that well-expressed areas with close-to-zero local divergence, which are also characteristic for dynamics with the slow passage effect, largely facilitate responses of a system to weak external forcing. For details, see subsection B. With this in mind, it is easy to understand that for the case studied here the steplike perturbation $f(t)$ reveals many additional UPOs that do not appear in the basic chaotic attractor [compare Figs. 5(a) and 5(b)].

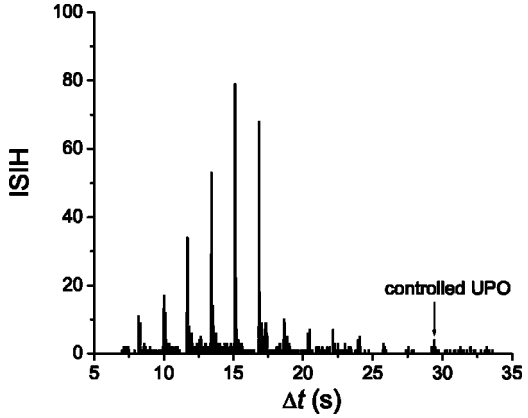

FIG. 6. Normalized ISIH of the c_{CaCyt} time series for the basic chaotic regime with the applied method. For equations and parameter values, see Appendix A.

In order to measure the multitude of additional UPOs obtained by our method, we calculate the ISIH for the perturbed dynamics of the system variable c_{CaCyt}. Results are presented in Fig. 6. By comparing Fig. 6 with Fig. 2, it is evident that the oscillation period distribution is much broader and continuous in the case of the perturbed dynamics than in the unperturbed case, approximately $7\ \mathrm{s} < T < 33\ \mathrm{s}$. It should be noted, however, that the predominant oscillation period remains $T \approx 15$ s, which shows that the basic system dynamics was not altered due to perturbations.

Now we show that the additional UPOs that are not part of the basic attractor can be controlled as easily, i.e., with very small correction fluxes added to the basic dynamics, as the UPOs that form the skeleton of the basic attractor. We choose an UPO with an oscillation period $T = 29.1$ s (marked with an arrow in Fig. 6), which lies far outside the oscillation period interval of UPOs that can be found in the basic chaotic attractor (see Fig. 2), additionally, the chosen UPO appears quite rare even in the perturbed time series. The results showing the control of the chosen UPO are presented in Fig. 7. It can be well observed that the system can easily shadow the selected UPO with control fluxes of the same order of magnitude as in the case of controlling UPOs from the unperturbed chaotic attractor (compare Figs. 3 and 7). In both cases the maximal required control flux is three orders of magnitude smaller than the total dc_{CaCyt}/dt flux (not shown). Moreover, the control is practically required only at the time the main c_{CaCyt} spike occurs, whereas during the small-amplitude spikes the required corrections are minute as shown in the inset of Fig. 7(b).

At the end, let us test the method for detecting additional UPOs on an example of a rigid intermittent chaotic behavior that can be found in the mathematical model proposed by Shen and Larter [18]. We studied this model previously [8,25] and found that the outlay of the local divergence oscillates heavily around zero with several well-expressed negative dells [8], which is characteristic for a rigid system. The rigidity of the system can also be well demonstrated with the fast-slow subsystem analysis performed as described in subsection A. In the examined dynamical system, the fast changing variables were identified to be c_{CaCyt} and

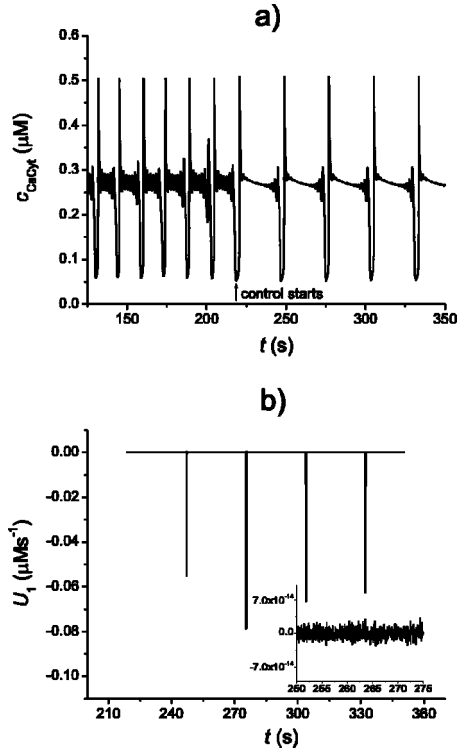

FIG. 7. Control of the unstable periodic orbit marked with an arrow in figure 6. For equations and parameter values, see Appendix A. (a) Time series of c_{CaCyt}. (b) The corrections required for controlling the desired UPO.

c_{IP}, whereas the slow changing variable, which is used as the bifurcation parameter, is c_{CaEr}. The obtained bifurcation diagram for the unperturbed dynamics, together with the 2D projection of the trajectory in the whole phase space, is presented in Fig. 8. It can be well observed that the trajectory is caught between two stable node branches (solid lines), whereas the transitions between the two are determined by the two fold bifurcations (up triangles). There is no sign of any slow passage effect. The trajectory is tied to one of the two stable branches most of the oscillation cycle, thereby

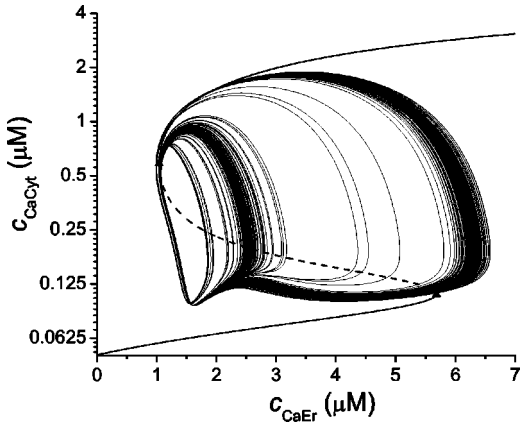

FIG. 8. Bifurcation diagram obtained with the fast-slow subsystem analysis together with the 2D projection of the trajectory in the whole phase space. For equations and parameter values, see Appendix B.

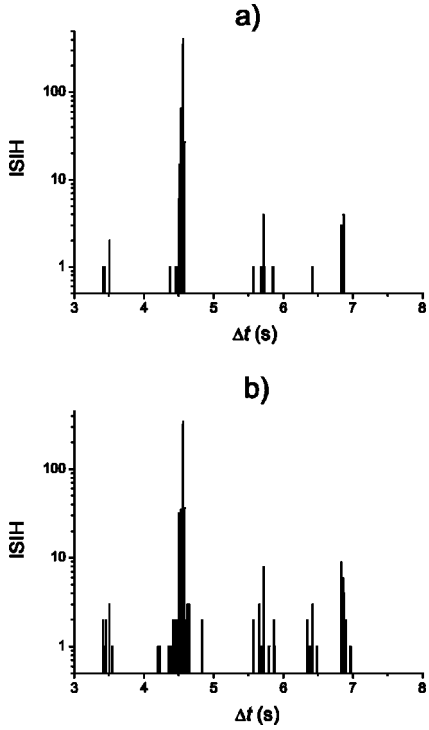

FIG. 9. Normalized ISIH of the c_{CaCyt} time series. For equations and parameter values, see Appendix B. (a) Basic chaotic regime. (b) Basic chaotic regime with the applied method. Note that the y axis has a logarithmic scale.

making it nearly impossible to achieve any noticeable deviations with the external perturbation.

For perturbing the examined dynamical system [18] by $f(t)$, we take the following intervals from which h, d, and a are chosen randomly: $30\ \mathrm{s}<h<40\ \mathrm{s}$, $0\ \mathrm{s}<d<1\ \mathrm{s}$, and $0\ \mu\mathrm{M\ s}^{-1}<a<4\ \mu\mathrm{M\ s}^{-1}$. We calculate ISIHs for the unperturbed and for the perturbed dynamics of the system variable c_{CaCyt} [Figs. 9(a) and 9(b), respectively]. Both histograms were calculated for approximately 10 000 main spikes. From the ISIH calculated for the perturbed dynamics [Fig. 9(b)] it is evident that the oscillation period distribution remained nearly unaffected by the applied method, which is a clear indicator that the examined chaotic attractor is very rigid [compare Figs. 9(a) and 9(b)]. It should be noted that the multitude of additional UPOs is small in spite the fact that we have chosen parameters d and a in Eq. (7) so that the system was perturbed maximally. For example, if we set $a=5\ \mu\mathrm{M\ s}^{-1}$, the system collapsed immediately.

Our results show that the method for detecting and controlling additional UPOs that are not part of the basic chaotic attractor is applicable to any chaotic system. It should be noted, however, that the multitude of additional UPOs detected depends on the flexibility of the system. In particular, the multitude of additional UPOs is much larger in case of a flexible attractor, whereas for a rigid attractor it might turn out that the number of additional UPOs is rather small.

IV. DISCUSSION

In the paper, a method for detecting and controlling UPOs that were not possible to control before is presented. These

additional UPOs are not part of the basic chaotic attractor. They can nevertheless be controlled as easily as the traditional UPOs of the system. The method exploits flexible parts of the attractor, which under weak external perturbation enable considerable deviations of the trajectory away from its originally determined path. The main idea is to temporarily destabilize the system and after the perturbation to wait for a natural resettling of the trajectory onto the basic chaotic attractor. During the resettling, which is defined by the same deterministic equations that form the attractor of the unperturbed dynamics, the trajectory moves through phase space areas that are normally not visited in the unperturbed case. Thereby, additional UPOs become visible and available for control. The frequency interval occupied by these UPOs is often considerably wider than the frequency range containing UPOs of the basic chaotic attractor. Our method can thus greatly increase the repertoire of genuinely diverse dynamical states that are available for control and herewith extends the applicability of traditional chaos control techniques.

The key system property that determines the flexibility of a dynamical system, and thereby the range to which a particular frequency interval containing UPOs of the basic chaotic attractor can be expanded, is the local divergence [15–17,35]. In order to point out the important role of the local divergence, we tested our method on two different mathematical models [14,18] that differ considerably in their flexibility. When the method was applied to the more flexible system [14], the multitude of additional UPOs was very large and the frequency interval of the UPOs expanded extensively. On the other hand, when the method was applied to the rigid system [18] additional UPOs could be found only in a moderate extension of the frequency interval that contains the UPOs of the basic chaotic attractor.

Recently, various chaos control techniques have been used not just to regularize chaotic behavior but also to control regular systems that are subjected to noise [10–12,36]. Our method has some similarities with controlling the behavior of noisy systems since, in both cases, the dynamics of the system is externally perturbed. It should be noted, however, that in noisy systems the noise acts continuously on the system, whereas our method is based on short pulsatile forcing that is applied intermittently [see Eq. (7)]. Thus, in our case, the controlled system is still autonomous in the sense that the perturbation is required only to make the additional UPOs visible, whereas the actual control starts after the perturbation. However, since noisy (nonautonomous) systems can be successfully controlled with external feedback techniques [11], our method can be applied to them as well. More precisely, with the proposed method the basic idea of controlling noisy oscillations [36] as well as noise-induced oscillations emerging from initially nonoscillatory regimes [10,11] is extended to the control of additional UPOs that can be found by temporarily destabilizing a chaotic system. Since the local divergence of attractors is the crucial system property that determines the response of a system to noise [15,16] and pulsatile forcing [17], it can be used for estimating the richness of additional dynamical states that can be made available for control due to any kind of external perturbations.

Since the seminal work of Ott *et al.* [2], chaos control techniques have been applied in various fields of research from physics, biology, chemistry, medicine, and economics [37–39]. Particularly in the field of nonlinear optics and laser technology, the need for stabilizing the irregular intensity fluctuations due to nonlinear couplings of several longitudinal and transverse modes [40] has been present from the very beginning of development. Accordingly, several works have been devoted to the control of chaos in lasers [41–47]. Especially in the case of controlling nonautonomous lasers [43,44,46,47], we see a possible implementation of our method, since the intracavity electro-optic crystal of the laser is already driven by an external sinusoidal or periodic impulsive voltage in order to modulate the cavity losses. Thus, by modifying the external voltage in accordance with our method, the behavior of the laser could be temporarily destabilized in order to evoke a new, perhaps more desirable, operation state, which could then be controlled and maintained with the same methods and techniques as the basic operation mode.

More recently, nonlinear optics and laser technology have also been used for information encoding [48,49] and digital communication [50,51]. In several studies [52–55], it has been shown that chaos control techniques can be used to provide a secure information flow between a sender and a receiver. In this context, our method could prove to be useful since it enables the acquisition of new dynamical states that can be used as additional digital information sources [56,57]. Because these states are not used by the unperturbed dynamics, a possible spy has basically no possibilities to reconstruct the underlying dynamics of a signal and decode the message. On the other hand, the required external perturbations that are necessary to make these additional dynamical states available as information sources, and later visible to the receiver, are very simple [see Eq. (7)] and can thus be encoded very efficiently with low powered microelectronic elements.

Another field of research that has benefited considerably from the chaos control theory is the biomedical engineering. Following the pioneering experiment in this field from Garfinkel *et al.* [58], chaos control techniques were used to control noisy neuronal activities [36], epileptiform bursting [59], and even to anticontrol the periodic behavior observed during an epileptic seizure [60]. Moreover, it has been suggested that certain chaos control techniques could be successfully implemented in biological pacemakers, which would not impose its own frequency, but would re-adjust its frequency in accordance with the system needs [47]. Since it is often the case that internal parameters of real-life biological systems cannot be changed, the method proposed here provides a good alternative to noninvasively detect and control UPOs that possibly assure optimal functionality of the tissue. Note that the method is noninvasive insofar that additional UPOs can be detected without changing the internal parameter values of the system.

In conclusion, with the proposed method, a wealth of genuinely new dynamical states, accessible with extremely small control influences to the basic dynamics, can be detected and controlled. The method is general and can be applied to any chaotic system; nevertheless, the system needs to be flexible, i.e., susceptible to external perturbations, in order to enable a productive implementation of the method.

In further studies, we are going to examine nonchaotic, yet flexible, dynamical systems in order to determine if there as well a hidden wealth of dynamical states outside the basic attractor can be found.

APPENDIX A

The mathematical model proposed by Marhl *et al.* [14] is described by the following differential equations:

$$\frac{dc_{\mathrm{CaCyt}}}{dt} = J_{\mathrm{ch}} - J_{\mathrm{pump}} + J_{\mathrm{leak}} + J_{\mathrm{out}} - J_{\mathrm{in}} + J_{\mathrm{CaPr}} - J_{\mathrm{Pr}}, \tag{A1}$$

$$\frac{dc_{\mathrm{CaEr}}}{dt} = \frac{\beta_{\mathrm{er}}}{\rho_{\mathrm{er}}}(J_{\mathrm{pump}} - J_{\mathrm{ch}} - J_{\mathrm{leak}}), \tag{A2}$$

$$\frac{dc_{\mathrm{CaMit}}}{dt} = \frac{\beta_{\mathrm{m}}}{\rho_{\mathrm{m}}}(J_{\mathrm{in}} - J_{\mathrm{out}}), \tag{A3}$$

where

$$J_{\mathrm{ch}} = k_{\mathrm{ch}}\frac{c_{\mathrm{CaCyt}}^2}{c_{\mathrm{CaCyt}}^2 + K_1^2}(c_{\mathrm{CaEr}} - c_{\mathrm{CaCyt}}), \tag{A4}$$

$$J_{\mathrm{pump}} = k_{\mathrm{pump}}c_{\mathrm{CaCyt}}, \tag{A5}$$

$$J_{\mathrm{leak}} = k_{\mathrm{leak}}(c_{\mathrm{CaEr}} - c_{\mathrm{CaCyt}}), \tag{A6}$$

$$J_{\mathrm{Pr}} = k_{+}c_{\mathrm{CaCyt}}c_{\mathrm{Pr}}, \tag{A7}$$

$$J_{\mathrm{CaPr}} = k_{-}c_{\mathrm{CaPr}}, \tag{A8}$$

$$J_{\mathrm{in}} = k_{\mathrm{in}}\frac{c_{\mathrm{CaCyt}}^8}{c_{\mathrm{CaCyt}}^8 + K_2^8}, \tag{A9}$$

$$J_{\mathrm{out}} = \left(k_{\mathrm{out}}\frac{c_{\mathrm{CaCyt}}^2}{c_{\mathrm{CaCyt}}^2 + K_1^2} + k_{\mathrm{m}}\right)c_{\mathrm{CaMit}}. \tag{A10}$$

$$c_{\mathrm{Pr}} = c_{\mathrm{PrTot}} - c_{\mathrm{CaPr}}, \tag{A11}$$

$$c_{\mathrm{CaPr}} = c_{\mathrm{CaTot}} - c_{\mathrm{CaCyt}} - \frac{\rho_{\mathrm{er}}}{\beta_{\mathrm{er}}}c_{\mathrm{CaEr}} - \frac{\rho_{\mathrm{m}}}{\beta_{\mathrm{m}}}c_{\mathrm{CaMit}}. \tag{A12}$$

Parameters values, if not stated otherwise, are $k_{\mathrm{ch}} = 4230\ \mathrm{s}^{-1}$, $k_{\mathrm{leak}} = 0.05\ \mathrm{s}^{-1}$, $k_{\mathrm{pump}} = 20\ \mathrm{s}^{-1}$, $k_{\mathrm{in}} = 300\ \mu\mathrm{M\ s}^{-1}$, $k_{\mathrm{out}} = 125\ \mathrm{s}^{-1}$, $k_{\mathrm{m}} = 0.00625\ \mathrm{s}^{-1}$, $k_{+} = 0.1\ \mu\mathrm{M}^{-1}\mathrm{s}^{-1}$, $k_{-} = 0.01\ \mathrm{s}^{-1}$, $K_1 = 5.0\ \mu$M, $K_2 = 0.8\ \mu$M, $c_{\mathrm{PrTot}} = 90\ \mu$M, $c_{\mathrm{CaTot}} = 120\ \mu$M, $\rho_{\mathrm{er}} = 0.01$, $\beta_{\mathrm{er}} = 0.0025$, $\rho_{\mathrm{m}} = 0.01$, $\beta_{\mathrm{m}} = 0.0025$.

APPENDIX B

The mathematical model proposed by Shen and Larter [18] is described by the following differential equations:

$$\frac{dc_{\mathrm{CaCyt}}}{dt} = J_{\mathrm{ch}} + J_{\mathrm{leak}} - J_{\mathrm{pump}} + J_{\mathrm{in}} - J_{\mathrm{out}}, \tag{B1}$$

$$\frac{dc_{\mathrm{CaEr}}}{dt} = J_{\mathrm{pump}} - J_{ch} - J_{\mathrm{leak}}, \tag{B2}$$

$$\frac{dc_{\mathrm{IP}}}{dt} = J_{+} - J_{-}, \tag{B3}$$

where

$$J_{\mathrm{ch}} = k_{\mathrm{ch}}\left(\frac{c_{\mathrm{IP}}^4}{c_{\mathrm{IP}}^4 + K_1^4}\right)\left(\frac{K_4 c_{\mathrm{CaCyt}}}{(c_{\mathrm{CaCyt}} + K_4)(c_{\mathrm{CaCyt}} + K_5)}\right)^3 c_{\mathrm{CaEr}}, \tag{B4}$$

$$J_{\mathrm{leak}} = k_{\mathrm{leak}}c_{\mathrm{CaEr}}, \tag{B5}$$

$$J_{\mathrm{pump}} = k_{\mathrm{pump}}\frac{c_{\mathrm{CaCyt}}^2}{c_{\mathrm{CaCyt}}^2 + K_2^2}, \tag{B6}$$

$$J_{\mathrm{in}} = k_{\mathrm{in1}}\, r + k_{\mathrm{in2}}, \tag{B7}$$

$$J_{\mathrm{out}} = k_{\mathrm{out}}\, c_{\mathrm{CaCyt}}, \tag{B8}$$

$$J_{+} = k_{+}r\frac{c_{\mathrm{CaCyt}}}{c_{\mathrm{CaCyt}} + K_3}, \tag{B9}$$

$$J_{-} = k_{-}c_{\mathrm{IP}}. \tag{B10}$$

Parameters values, if not stated otherwise, are $k_{\mathrm{ch}} = 3000\ \mu\mathrm{M\ s}^{-1}$, $k_{\mathrm{leak}} = 1.0\ \mathrm{s}^{-1}$, $k_{\mathrm{pump}} = 50.0\ \mu\mathrm{M\ s}^{-1}$, $k_{\mathrm{in1}} = 4.0\ \mu\mathrm{M\ s}^{-1}$, $k_{\mathrm{in2}} = 1.0\ \mu\mathrm{M\ s}^{-1}$, $k_{\mathrm{out}} = 10.0\ \mathrm{s}^{-1}$, $k_{+} = 4.0\ \mu\mathrm{M\ s}^{-1}$, $k_{-} = 2.0\ \mu\mathrm{M\ s}^{-1}$, $K_1 = K_2 = 0.2\ \mu$M, $K_3 = 1.0\ \mu$M, $K_4 = K_5 = 0.69\ \mu$M, $r = 0.62$.

[1] E. N. Lorenz, J. Atmos. Sci. **20**, 130 (1963).
[2] E. Ott, C. Grebogi, and J. A. Yorke, Phys. Rev. Lett. **64**, 1196 (1990).
[3] E. R. Hunt, Phys. Rev. Lett. **67**, 1953 (1991).
[4] K. Pyragas, Phys. Lett. A **170**, 421 (1992).
[5] S. Boccaletti and F. T. Arecchi, Europhys. Lett. **31**, 127 (1995).
[6] B. B. Plapp and A. W. Huebler, Phys. Rev. Lett. **65**, 2302 (1990).
[7] R. Lima and M. Pettini, Phys. Rev. A **41**, 726 (1990).
[8] M. Perc and M. Marhl, Biophys. Chem. **104**, 509 (2003).
[9] Y. Braiman and J. Goldhirsch, Phys. Rev. Lett. **66**, 2545 (1991).
[10] L. Gammaitoni *et al.*, Phys. Rev. Lett. **82**, 4574 (1999).
[11] J. Lindner *et al.*, Phys. Rev. E **63**, 041107 (2001).
[12] D. Goldobin, M. Rosenblum, and A. Pikovsky, Phys. Rev. E

67, 061119 (2003).
[13] T. Haberichter, M. Marhl, and R. Heinrich, Biophys. Chem. **90**, 17 (2001).
[14] M. Marhl, T. Haberichter, M. Brumen, and R. Heinrich, BioSystems **57**, 75 (2000).
[15] M. Perc and M. Marhl, Phys. Lett. A **316**, 304 (2003).
[16] M. Perc and M. Marhl, Physica A **332**, 123 (2004).
[17] M. Perc and M. Marhl, Bioelectrochem. Bioenerg. **62**, 1 (2004).
[18] P. Shen and R. Larter, Cell Calcium **17**, 225 (1995).
[19] E. Doedel, A. Champneys, T. Fairgrieve, and Y. Kuznetsov, *AUTO97: Continuation and Bifurcation Software for Ordinary Differential Equations* (Concordia University, Montreal, 1997).
[20] J. Rinzel, in *Ordinary and Partial Differential Equations. Lecture Notes in Mathematics, Berlin, 1985*, edited by B. D. Sleeman and R. J. Jarvis (Springer-Verlag, Berlin, 1985), p. 304.
[21] M. Marhl and S. Schuster, J. Theor. Biol. **224**, 491 (2003).
[22] S. Boccaletti and F. T. Arecchi, Physica D **96**, 9 (1996).
[23] F. T. Arecchi and S. Boccaletti, Chaos **7**, 621 (1997).
[24] S. Boccaletti, A. Farini, and F. T. Arecchi, Chaos, Solitons Fractals **8**, 1431 (1997).
[25] M. Perc and M. Marhl, Chaos, Solitons Fractals **18**, 759 (2003).
[26] M. Perc and M. Marhl, Chem. Phys. Lett. **376**, 432 (2003).
[27] S. M. Baer, T. Erneux, and J. Rinzel, SIAM (Soc. Ind. Appl. Math.) J. Appl. Math. **49**, 55 (1989).
[28] A. Nejshtadt, Usp. Mat. Nauk **40**, 190 (1985).
[29] L. Holden and T. Erneux, SIAM (Soc. Ind. Appl. Math.) J. Appl. Math. **53**, 1045 (1993).
[30] L. Holden and T. Erneux, J. Math. Biol. **31**, 351 (1993).
[31] E. M. Izhikevich, SIAM (Soc. Ind. Appl. Math.) J. Appl. Math. **60**, 503 (2000).
[32] E. M. Izhikevich, Int. J. Bifurcation Chaos Appl. Sci. Eng. **10**, 1171 (2000).
[33] E. M. Izhikevich, SIAM Rev. **43**, 315 (2001).
[34] J. Rinzel and M. Baer, Biophys. J. **54**, 551 (1988).
[35] M. Perc and M. Marhl, Int. J. Bifurcation Chaos Appl. Sci. Eng. in press.
[36] D. J. Christini and J. J. Collins, Phys. Rev. Lett. **75**, 2782 (1995).
[37] F. T. Arecchi *et al.*, Int. J. Bifurcation Chaos Appl. Sci. Eng. **8**, 1643 (1998).
[38] S. Boccaletti *et al.*, Phys. Rep. **329**, 103 (2000).
[39] J. A. Holyst and K. Urbanowicz, Physica A **287**, 587 (2000).
[40] C. Bracikovski and R. Roy, Chaos **1**, 49 (1991).
[41] R. Roy, T Murphy, T. Maier, and Z. Gills, Phys. Rev. Lett. **68**, 1259 (1992).
[42] S. Bielawski, D. Derozier, and P. Glorieux, Phys. Rev. E **49**, 971 (1994).
[43] R. Meucci, M. Ciofini, and R. Abbate, Phys. Rev. E **53**, 5537 (1996).
[44] M. Ciofini, A. Labate, and R. Meucci, Phys. Lett. A **227**, 31 (1997).
[45] R. Meucci, A. Labate, and M. Ciofini, Phys. Rev. E **56**, 2829 (1997).
[46] M. Basso, R. Genesio, M. Stanghini, and A. Tesi, Chaos, Solitons Fractals **8**, 1449 (1997).
[47] F. T. Arecchi, R. Meucci, A. Di Garbo, and E. Allaria, Opt. Lasers Eng. **39**, 293 (2003).
[48] P. M. Alsing *et al.*, Phys. Rev. E **56**, 6302 (1997).
[49] I. P. Marino *et al.*, Chaos **13**, 286 (2003).
[50] G. D. Van Wiggeren and R. Roy, Phys. Rev. Lett. **81**, 3547 (1999).
[51] G. D. Van Wiggeren and R. Roy, Int. J. Bifurcation Chaos Appl. Sci. Eng. **9**, 2129 (1999).
[52] L. M. Pecora and T. L. Carroll, Phys. Rev. Lett. **64**, 821 (1990).
[53] M. Ding and E. Ott, Phys. Rev. E **49**, 945 (1994).
[54] J. H. Peng, E. J. Ding, M. Ding, and W. Yang, Phys. Rev. Lett. **76**, 904 (1996).
[55] S. Boccaletti, A. Farini, and F. T. Arecchi, Phys. Rev. E **55**, 4979 (1997).
[56] S. Hayes, C. Grebogi, E. Ott, and A. Mark, Phys. Rev. Lett. **70**, 3031 (1993).
[57] S. Hayes, C. Grebogi, E. Ott, and A. Mark, Phys. Rev. Lett. **73**, 1781 (1994).
[58] A. Garfinkel, M. Spano, W. Ditto, and J. Weiss, Science **257**, 1230 (1992);
[59] M. W. Slutzky, P. Cvitanovic, and D. J. Mogul, IEEE Trans. Biomed. Eng. **50**, 559 (2003).
[60] S. J. Schiff *et al.*, Nature (London) **370**, 615 (1994).